Synthesis and magnetic properties of the multiferroic $GaFeO_3$ of orthorhombic and hexagonal symmetry

K. REĆKO[a*], U. WYKOWSKA[b], W. OLSZEWSKI[c], G. ANDRÉ[d], J.J. MILCZAREK[e], D. SATUŁA[a], M. BIERNACKA[a], B. KALSKA-SZOSTKO[b], J. WALISZEWSKI[a], K. SZYMAŃSKI[a]
[a]*Faculty of Physics, University of Bialystok, K. Ciołkowskiego 1L, 15-245 Białystok, Poland*
[b]*Institute of Chemistry, University of Bialystok, K. Ciołkowskiego 1K, 15-245 Białystok, Poland*
[c]*ALBA Synchrotron Light Source, Ctra. BP 1413 km. 3,3, 08290, Cerdanyola del Valle`s, Barcelona, Spain*
[d]*Laboratoire Léon Brillouin, CEA-Saclay, 91191 Gif sur Yvette cedex*
[e]*National Centre for Nuclear Research, A. Sołtana 7, 05-400 Otwock, Świerk, Poland*

In the past decade research on the multiferroic nature of gallium iron oxide has been of interest for several reasons. $GaFeO_3$ (GFO) has been intensively studied for its potential applications as a magnetoelectric material [1]. Such a system can be used for switching its electric state vs. magnetic state and vice versa. Moreover GFO seems to be promising memory media which allow a simultaneous reading and writing of data and will be useful in data storage as well [2]. The physical properties especially magnetism in $GaFeO_3$, depend strongly on the method of preparation. This work reports the preparation of gallium iron oxide by the sol–gel route (SG) and its characterization made by x-ray together with neutron diffraction techniques. The low- and room temperature ^{57}Fe Mössbauer spectroscopy measurements were collected to complement the phase characteristics with relative fractions of the orthorhombic end/or hexagonal phases.

(Received May 7, 2015; accepted June 24, 2015)

Keywords: 61.12.-q Neutron diffraction, 61.18.Fs Mössbauer spectroscopy, Nanoparticles 81.07.-b, Sol-gel 81.05.-t

1. Introduction

Many efforts have been expended on fabrication of gallium iron oxide by Pechini modification of the sol-gel method, which offers the possibility to synthetize multifunctional material. Moreover, the choice of SG synthesis was dictated by the possibility of obtaining the very small grains (from ~70 nm [3] up to 15 nm). According to a scenario we should use $Ga(NO_3)_3 \cdot 6H_2O$ [4] or dissolving metallic gallium in 10% solution of HNO_3 until to obtain the aqueous $Ga(NO_3)_3$ as a semiproduct reacts with a stoichiometric amount of $FeCl_3 \cdot 6H_2O$ in an environment of aqua distillate, citric acid (CA) and ethyl glycol (EG). According to our best knowledge the perfectly ordered gallium iron oxide of an atomic ratio 1:1:3 is able to crystallize in an orthorhombic crystal structure only. The crystallographic unit cell contains 4 different cation sites and 6 oxygen anion sites all in general position (4a: x, y, z) of the $Pc2_1n$ space group (no. 33). In the perfectly ordered structures, as shown in Fig. 1, sites labeled by Ga(1) – is an unique and sole tetrahedral one, Ga(2), and Fe(1), Fe(2) are octahedral ones and all four entirely occupied by Ga^{3+} and by Fe^{3+} ions, respectively. In such a case, there is no chance to form uncompensated antiferromagnetism thanks to which spontaneous electric polarization could be steered.

Such simple and effective mechanism works in so called switch materials with non-centrosymmetric chemical units, which contain the magnetic ions and simultaneously can become an origin of ferroelectricity.

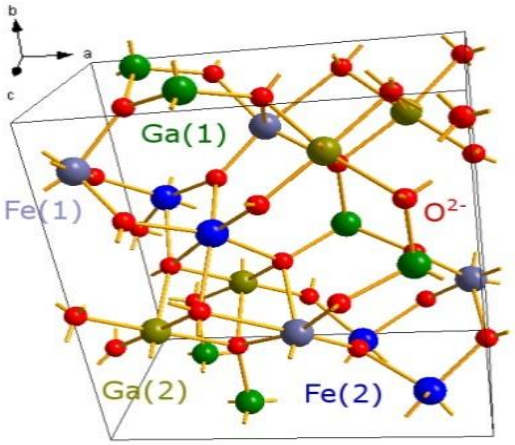

Fig. 1 Orthorhombic structure of well-ordered $GaFeO_3$ sample with the room temperature lattice parameters $a \approx 870$ pm, $b \approx 940$ pm and $c \approx 507$ pm.

Magnetically, the orthorhombic system forms a collinear antiferromagnetic ordering along [001] direction with the calculated magnetic moment of irons reaching up to the values of even $5\mu_B$ per atom [5]. Any disorder of the cations origin leads to more complicated non-collinear structures. So far for systems GFO the ferromagnetism [6], canted antyferromagnetyzm [7] or ferrimagnetism [8, 9] were reported. In the light of neutron diffraction and Mössbauer measurements the strong correlation of the

magnetic ordering against the cation distribution among the sites has been proven [10].

Moreover, according to Authors [11] the normal conditions of the temperature and pressure in the wide range of compositions x ϵ <0.7, 1.4> of $Ga_{2-x}Fe_xO_3$ favor orthorhombic ($Pc2_1n$) crystal order. The oxygen anions therein pack in quasi-hexagonal layers with double – hexagonal close packed type repetitions. Whereas, at starting high temperature close to 900^0C and pressure of 40 kbar during quenching process up to room conditions of temperature and pressure the new phase – isostructural with α - corundum – α - $(Ga,Fe)_2O_3$ was obtained. In consequence all gallium cations reached the coordination number equal to 6. The crystallographic unit cell of α-Fe_2O_3 contains 2 sites only. The oxygen ions locate at *18e*: (x,0,1/4), while *12c*: (0,0,z) are occupied by iron ones. Simultaneously, due to the similarity of ionic radius of Fe^{3+} (64,5 pm) and Ga^{3+} (62 pm) the changes of unit cell parameters can be unnoticeable during X-ray diffraction in contrast to the other kinds of in-site disordering or oxygen vacancies regarding large ionic radius of O^{2-} (140 pm).

The authors of this paper wish to propose the simple preparation at much lower temperatures and normal pressure which lead to synthesis the gallium iron oxides of hexagonal symmetry. The aim of this paper is observation how the targeted preparation allows for controlling the sample's homogeneity, their chemical order and – in consequence – the distribution of the magnetic ions and the saturation magnetization at high temperatures.

2. Preparation procedures

Three various scenarios were adopted on fabrication of gallium iron oxide (see Table 1). During preparation acids concentrations, the ratio of (CA+EG) environment according to Pechini modification as well as the annealing temperatures have been optimized. Finally isostructural gallium iron oxides which crystallize with different symmetry were obtained (Fig. 3). The synthesis carried out in accordance with the standard procedure of SG where gallium nitrate (III) is a semiproduct allows for obtaining single phase of the GFO with orthorhombic symmetry of $Pc2_1n$ space group, while the same procedure with the semiproduct of gallium chloride (III) leads to a single phase $GaFeO_3$ composition of corundum type - hexagonal symmetry of R3c (see Fig. 2 and Fig. 3-lower panel).

Table 1. Preparation procedures of $Ga_{(1-x)}Fe_{(1+x)}O_3$ nanoparticles.

Sample 1 Orthorhombic +Hexagonal High Temerature Heating HTH	Sample 2 Orthorhombic Low Temerature Heating LTH	Sample 3 Hexagonal Low Temerature Heating LTH_CH
Ga +10% HNO_3 Semiproduct $Ga(NO_3)_3$ x nH_2O		Ga +10% HCl Semiproduct $GaCl_3$ x nH_2O
58.7 ml of (0.01 M) citric acid (CA) and 0.7 ml of ethylene glycol (EG) were added to a solution of hydrated gallium nitrate or hydrated gallium chloride		
The mixture was heated and stirred at 60^0C for 1hour		
Then the stoichiometric amounts of $FeCl_3$ x $6H_2O$ (99,9%) were added		
In order to evaporate the solvent the heating procedure was carried out at a constant temperature of 60^0C		
The gel was subjected to thermal decomposition at 400^0C to a dark brown powder, which was then annealed at 800^0C for 5hours	The gel was subjected to annealing procedure for 8 hours at the temperature of 200^0C, followed by 4 hours at 250^0C	
The powder was ground and further annealed at 900^0C for 10 hours	Additional heating steps: 600^0C for (1+3) hours 600^0C for 4h 400^0C for 4h	Additional heating step: 600^0C for 4 hours

3. Diffraction data analysis

XRD phase identification were performed by use SuperNova diffractometer at the room temperature with the KMo of wavelength 70.926 pm while the ND data were carried out on two-axis diffractometer G4-1 (LLB, Orphée) at the temperature range 1.8 - 299 K with the initial neutron beam of wavelength 242.3 pm monochromated by pyrolytic graphite (002) and DH-5 neutron diffractometer P (NCNR, Maria) with double–crystal monochromator Cu (200) and the neutron beam of wavelength 149.85 pm.

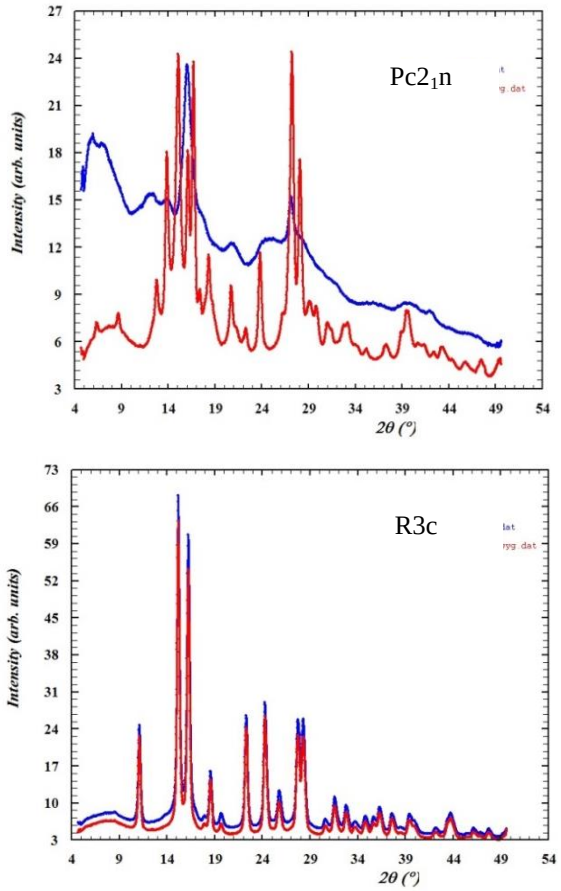

Fig. 2 X-ray diffraction patterns for orthorhombic and hexagonal samples before (blue diagrams) and after annealing (red diagrams).

The low temperature of the gel aging[1] and short annealing times effectively prevent the precipitation of hematite phase and facilitate the formation of smaller grains. It is worth noting that our previous structural investigations of $GaFeO_3$ compounds revealed a presence of mixed structural states Pc2$_1$n+R3c.

The prepared samples 2 and 3 are found to be single phase, while the sample 1 is biphasic (see Fig. 4). As a result of site-disorder at orthorhombic as well as at hexagonal symmetry, the occupation of Ga^{3+} in one of the Fe sites alters the strength of the exchange interaction between Fe^{3+} ions by changing the Fe–O–Fe bond parameters and hence gives the possibility of tuning the magnetic transition temperatures and spontaneous magnetization values. Thus, the estimation of the cation's distribution in each sublattice is necessary to understand the magnetic properties of $GaFeO_3$ system.

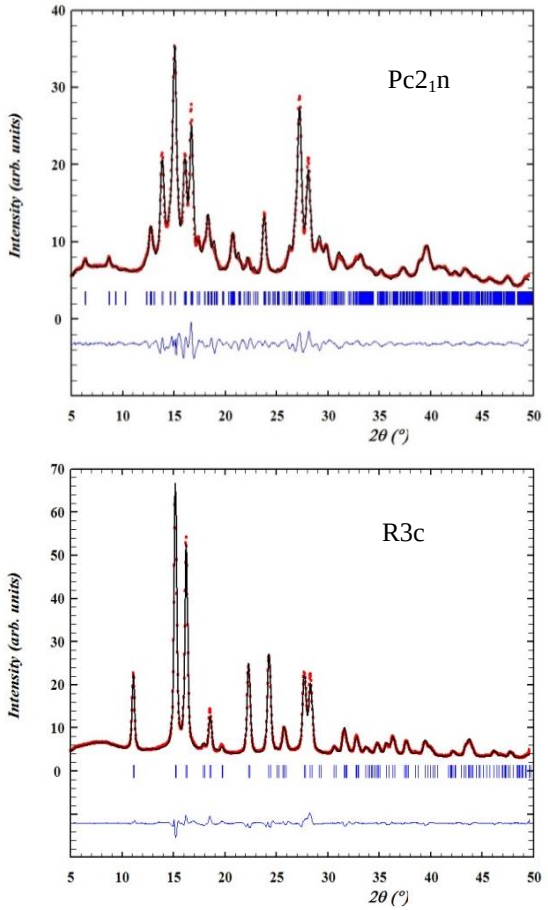

Fig. 3 The room temperature X-ray data refinement of single phase orthorhombic GFO – sample 2 (upper panel) and single phase hexagonal GFO – sample 3 (lower panel). The profile fitting (black lines) resulting from Rietveld refinement for patterns. The blue bars show the position of Bragg peaks of appropriate single phases. At the bottom in the figures, the difference plot, I_{obs}-I_{calc} (blue line), are shown.

[1]The aging procedure is used in order to evaporate the solvent the heating procedure was carried out at a constant temperature of 60^0C, while the time of aging depends on the sample consistency.

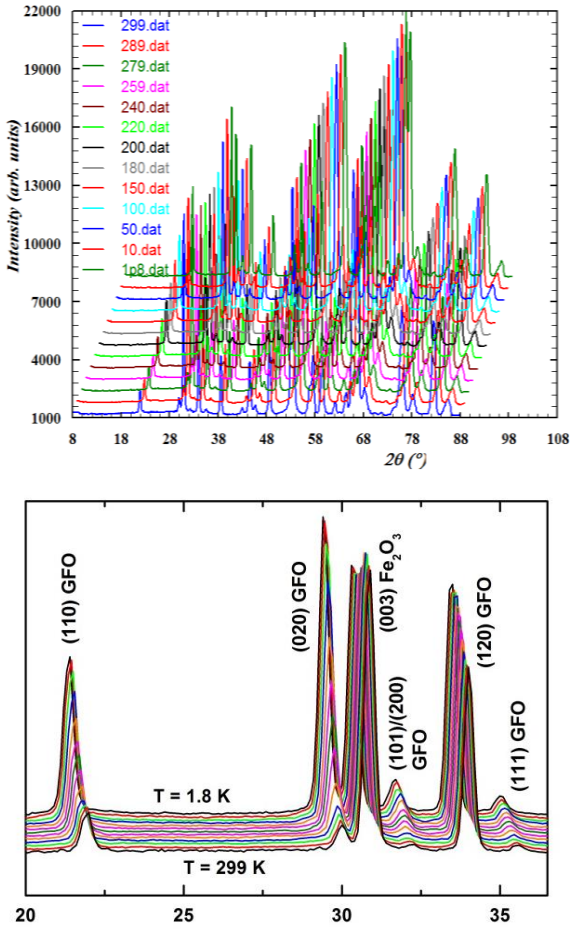

Fig. 4 Temperature behavior in the range of 1.8 K – 299 K of the biphasic sample 1 measured by use neutron spectrometer G4.1 (λ=242.3 pm) in the wide scattering angle range (upper panel) where the strongest magnetic reflections (110) and (020) are well visible up to 30 in the 2θ scale (lower panel).

Against the temperature decrease, the intensities of the orthorhombic phase GFO enhance substantially as a result of significant magnetic scattering contributions while the intensities of the reflections related to an extra hexagonal phase remain much weaker depend on temperature (see lower panel of Fig. 4). The resultant ion magnetic moment drops down by ~20% with the increasing temperature in the range 10-300 K (see 4th column of Table 2 and Fig. 5). It is fully consistent with high value of iron magnetic moment and well visible sextet collected during room temperature Mössbauer spectroscopy measurements presented at chapter 5.

On the other hand, powder pure hematite is antiferromagnetic below the Morin temperature (T_M) with the magnetic moment of the Fe^{2+}along [111] direction. Above T_M and below the Neel temperature (T_N ~ 955K), the iron ions spins lie in the (111) plane with a slight canting away from the perfect antiferromagnetic alignment [13]. Additionally, according to reported results [13] hematite nanoparticles have shown a suppression of the Morin transition and stay in the weakly ferromagnetic state down to 5K.

Different magnetic phase transition temperatures do not surprised due to quite different chemical order from sample to sample. At sample 1 three sublattices disclose almost the same mixed occupancy, namely Ga(2), Fe(1) and Fe(2) while in the sample 2 Ga(2) and Fe(1) sublattices only characterize similar resultant scattering amplitude and pure iron occupancy of Fe(2) positions.

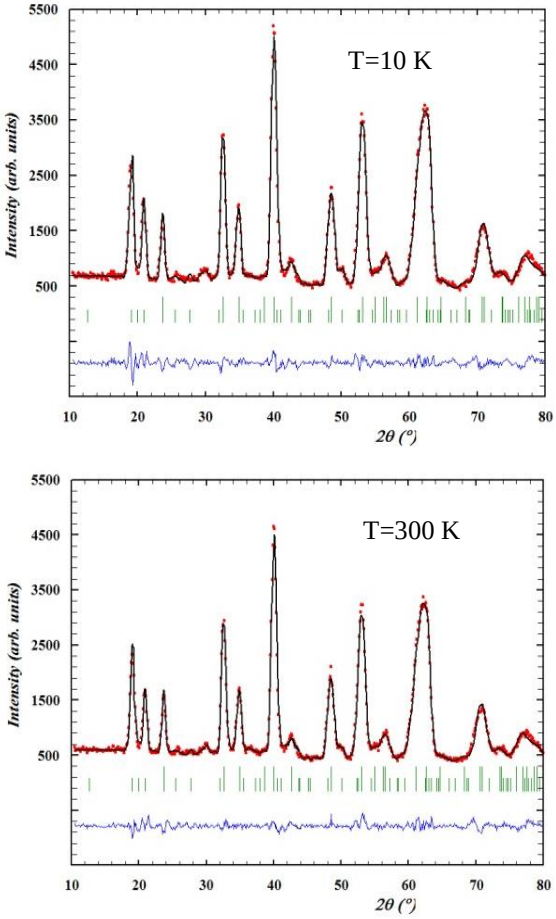

Fig. 5. Neutron diagrams collected on sample 3 - hexagonal GFO at 10 (upper panel) and 300 K (lower panel) by use DH-5 neutron diffractometer (λ=149.85 pm).

Table 2. Review of same properties of the $Ga_{(1+x)}Fe_{(1-x)}O_3$ samples i.e. the phase transition temperatures with the selected structural parameters. The diffraction patterns were analyzed by a Rietveld - type profile refinement method using FULLPROF program [12]. The stoichiometries of the samples were calculated from partial sites occupancies obtained at Neél temperatures (T_N).

Sample's number	Sample 1 $Pc2_1n$ + R3c	Sample 2 $Pc2_1n$	Sample 3 R3c
Composition	$Ga_{1.37}Fe_{0.63}O_3$	$GaFeO_3$	$GaFeO_3$
Site occupancy Fe/Ga	Ga(1) – 12/88(±9) Ga(2) – 35/65(±6) Fe(1) – 38/62(±6) Fe(2) – 41/59(±9)	Ga(1) – 5/95(±7) Ga(2) – 43/57(±4) Fe(1) – 52/48(±4) Fe(2) – 95/5(±7)	Fe(1) – 50/50(±3)
Extra phase	~ 18% $Fe_{1.67}Ga_{0.33}O_3$ R 3 c μFe ~ $2.3\mu_B/Fe^{3+}$		10 K μ_{Fe3} = 1.98(2) μ_B//[111] 300 K μ_{Fe3} = 1.57(4) μ_B//[111]
T_N	~260 K	~180K	
AF T = 1.8 K	μ_{Fe1} = 3.07(5) μ_B//[101]	10 K μ_{Fe2} = 3.97(2) μ_B//[101]	

In the case of HTH as well as LTH used during SG preparation the resultant iron magnetic moments lie in the [101] direction (see also Table 2). Moreover, the average grain size distributions are significantly different from 200 nm for sample 1 up to 15 nm for sample 2. Obviously, multiferroic system exhibits stronger switch properties in direct proportion to its finer grain size distribution, and paradoxically, for the same reason it quickly reaches superparamagnetic state.

4. Magnetization characteristics

The magnetization measurements were carried out using vibrating sample magnetometer (VSM) under magnetic fields up to 1.2 T in the temperature 10 K and 300 K, both with zero-field-cooling (ZFC) and field-cooling (FC) scenarios.

In the case of sample 2 the magnetic hysteresis loop measured at 10K is markedly wider (upper panel of Fig. 6), compared to sample 3 which indicates magnetically soft phase type of uncompensated antiferromagnetic hematite. The appropriate saturation magnetizations obtained for sample 2 are equal to $M_{s(10K)}$=0.353 μ_B, $M_{s(295K)}$=0.04 μ_B while for sample 3 – $M_{s(10K)}$=0.036 μ_B, $M_{s(295K)}$=0.02 μ_B, respectively. Noteworthy, the phase transitions temperatures estimated from FC and ZFC measurements curried out at 100 Oe are equal to 175 K for sample 2 and 240 K for sample 3. The last one weakly corresponds to the Morin temperature (T_M~263K), typical for pure hematite [13]. The competition between the iron spin arrangements favor plane parallel to c axis below T_M and the spin arrangements favor plane perpendicular to c axis above T_M as well as the mixed occupancy of the *(12c)* positions seems to be proper explanation of the much lower transition temperature of sample 3 and the fact that the Morin transition was not observed in the neutron data measurements carried out up to room temperature.

The coercive field H_C of sample 2 is more than 4 times higher than the coercive field of sample 3, which may indicates a strong magnetic anisotropy[2] of the sample 2. This feature seems to be very promising from point of view saturation magnetization at temperatures close to the room one. It is noteworthy, that at room temperature, both samples show a non-zero magnetic moment.

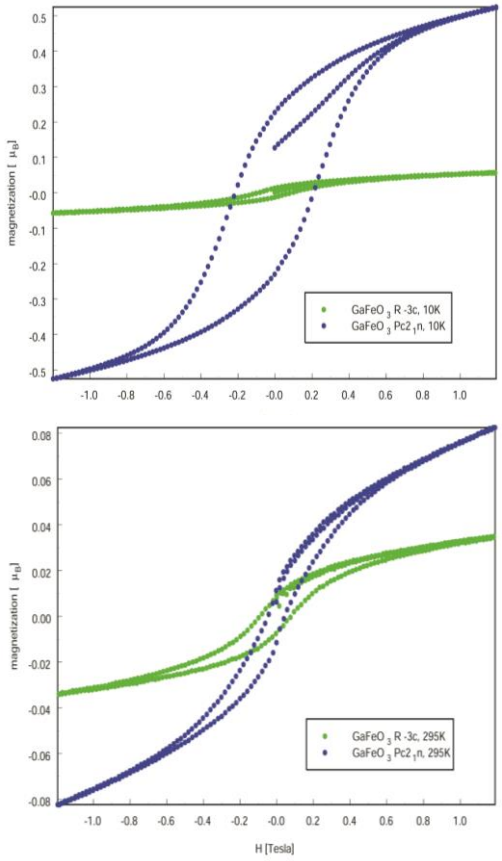

Fig. 6 Magnetization of the sample 2 (blue dots) and 3 (green dots) as a function of the external magnetic field at low (upper panel) and high temperature (lower panel).

5. Mössbauer data analysis

The Mössbauer spectra were collected in transmission geometry with a standard constant acceleration spectrometer and with the ^{57}Fe source in a Cr matrix. The

[2]Noteworthy, the typical for orthorhombic GFO is easy magnetization c axis, and (P_z) electric polarization vector along b axis. The last mentioned is directly related to crystal symmetry ($Pc2_1n$ => P_z > 0 (59 μC/cm^2); Pnna => P_z = 0; $Pna2_1$ => P_z < 0 (-24 μC/cm^2) [2] and strictly results from the Ga(1) – O bonds tilting with respect to b crystallographic parameter.

upper (sample 1) and middle (sample 3) Mössbauer spectra measured at RT show two components (see Fig. 7). The high temperature data were fitted as a superposition of components belong to gallium iron oxide and hematite. Sextet comes from Fe_2O_3 and doublet from paramagnetic state of GFO.

The spectrum in the middle disclosed circa 7 % - contribution of the orthorhombic phase – invisible in the diffraction data. The hyperfine field associated to the basic – hexagonal phase reaches 52T thus the iron magnetic moments is equal to $3.5\mu_B$/Fe atom. The lower Mössbauer spectrum belongs to pure orthorhombic GFO phase, where the analysis was carried out taking into account the three components, each of them corresponding to appropriate site of orthorhombic structure, what fully deals with the neutron results obtained for sample 2.

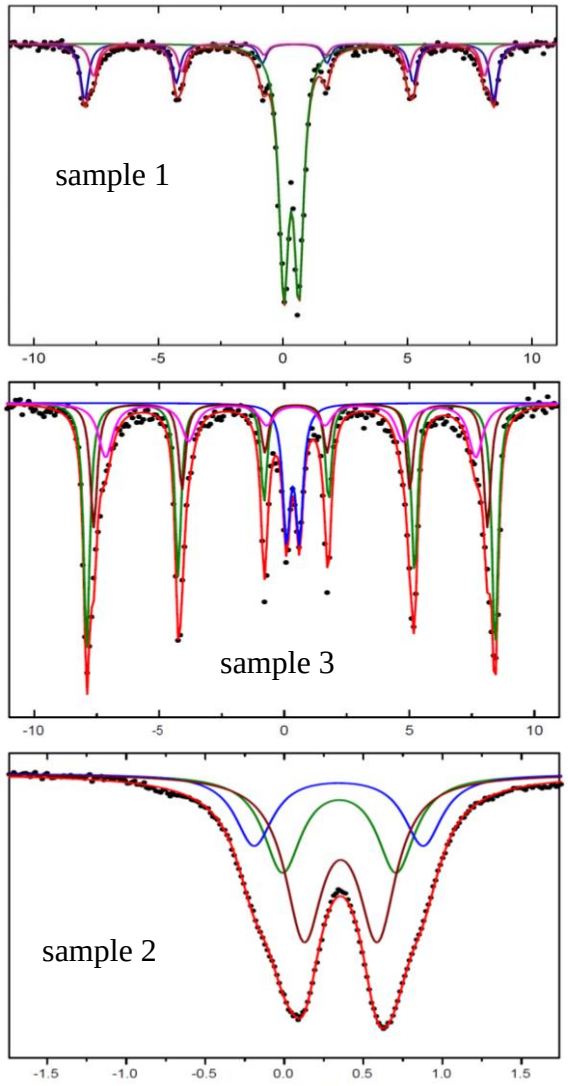

Fig. 7 Results of MS spectra fit with the impurity phase for sample 1 and 3 and for single phase - sample 2, respectively. All of the spectra were recorded at room temperature.

6. Remarks and conclusions

The type and concentration of gallium salt and low temperature aging gel influence on the homogeneity and chemical ordering as well as on indeed different occupancy of iron and gallium sites at GFO, and further modify the magnetic ordering. The symmetry of the basic phases is an orthorhombic and/or hexagonal one. The orthorhombic phase consists of three magnetic sublattices, due to in the case of samples 1 and 2 within the errors the Ga(1) positions are non-magnetic.

The different symmetries result in explicitly different magnetic behavior, i.e. temperatures of phase transitions, the fields of coercivity, saturation magnetization values, and the FC and ZFC characteristics (sample 2 and 3). The values of the resultant magnetic moments of iron cations are as follow: Fe ~ 3 μ_B // [101] (sample 1) and ~ 4 μ_B // [101] (sample 2) and close to 2 μ_B // [101] (sample 3). In the case of gallium doped hematite phase at 50% the resultant moment is close to Fe ~ 2.3 μ_B (sample 1), while almost pure $GeFeO_3$ which crystalizes at α-Fe_2O_3 structure discloses $2_{T=10K}$-1.5_{RT} μB (sample 3).

References

[1] R. Saha, A. Shireen, S.N. Shirodkar, U.V. Waghmare, A Sundaresan, C.N.R Rao, Solid State Communications **152** 1964 (2012).
[2] D. Stoeffler, J. Phys.: Condens. Matter **24** 185502 (2012).
[3] M. Bakr Mohamed, H. Wang and H. Fuess, J.Phys. D: Appl. Phys. **43** 455409 (2010).
[4] M. Bakr Mohamed, A. Senyshyn, H. Ehrenberg, H. Fuess, J. Alloys Comp. **492** (1-2) L20 (2010).
[5] M.J. Han, T. Ozaki, and J. Yu, Phys. Rev B. **75** 060404 (2007).
[6] J.P. Remeika, J. Appl. Phys. Suppl. **31**, 263S (1960).
[7] George T. Rado, Phys. Rev. Lett. **13**, 335 (1964).
[8] R. B. Frankel, N. A. Blum, S. Foner, A.J. Freeman M. Schieber, Phys. Rev. Lett. **15** 958 (1965).
[9] T. Arima, J. Phys.: Condens. Matter **20,** 434211 (2008).
[10] K. Rećko, K.Szymański, L. Dobrzyński, J. Waliszewski, Acta Physica Polonica A **122,** 396 (2012).
[11] M. Marezio and J.P. Remeika, J. Chem. Phys. **46(**5), 1862 (1967).
[12] J. Rodriguez-Carvajal, Phys. B **192,** 55 (1993).
[13] A.H. Morrish, Canted antiferromagnetism, Hematite, World Scientific, Singapore (1994).

*Corresponding author: k.recko@uwb.edu.pl